Received: 5 March 2020 | Revised: 2 May 2020 | Accepted: 11 May 2020

DOI: 10.1111/cas.14485

Cancer Science WILEY

ORIGINAL ARTICLE

Thymidylate synthase inhibitor raltitrexed can induce high levels of DNA damage in *MYCN*-amplified neuroblastoma cells

Ken Yamashita[1] | Shinichi Kiyonari[1,2] | Shoma Tsubota[1] | Satoshi Kishida[1] | Ryuichi Sakai[2] | Kenji Kadomatsu[1]

[1]Department of Biochemistry, Nagoya University Graduate School of Medicine, Nagoya, Japan

[2]Division of Biochemistry, Kitasato University School of Medicine, Sagamihara, Japan

Correspondence
Shinichi Kiyonari and Kenji Kadomatsu, Nagoya University Graduate School of Medicine, Nagoya, Japan.
Email: kiyonari@med.nagoya-u.ac.jp (SK); kkadoma@med.nagoya-u.ac.jp (KK)

Funding information
Japan Society for the Promotion of Science, Grant/Award Number: JP15K18442 and JP19K07711

Abstract

MYCN gene amplification is consistently associated with poor prognosis in patients with neuroblastoma, a pediatric tumor arising from the sympathetic nervous system. Conventional anticancer drugs, such as alkylating agents and platinum compounds, have been used for the treatment of high-risk patients with *MYCN*-amplified neuroblastoma, whereas molecule-targeting drugs have not yet been approved. Therefore, the development of a safe and effective therapeutic approach is highly desired. Although thymidylate synthase inhibitors are widely used for colorectal and gastric cancers, their usefulness in neuroblastoma has not been well studied. Here, we investigated the efficacies of approved antifolates, methotrexate, pemetrexed, and raltitrexed (RTX), on *MYCN*-amplified and nonamplified neuroblastoma cell lines. Cell growth-inhibitory assay revealed that RTX showed a superior inhibitory activity against *MYCN*-amplified cell lines. We found no significant differences in the protein expression levels of the antifolate transporter or thymidylate synthase, a primary target of RTX, among the cell lines. Because thymidine supplementation could rescue the RTX-induced cell growth suppression, the effect of RTX was mainly due to the reduction in dTTP synthesis. Interestingly, RTX treatments induced single-stranded DNA damage response in *MYCN*-amplified cells to a greater extent than in the non-amplified cells. We propose that the high DNA replication stress and elevated levels of DNA damage, which are a result of deregulated expression of *MYCN* target genes, could be the cause of increased sensitivity to RTX.

KEYWORDS

antifolate, chemotherapy, MYCN, neuroblastoma, raltitrexed

Abbreviations: ATM, ataxia telangiectasia mutated; ATR, ataxia telangiectasia and Rad3-related; BBB, blood brain barrier; Chk, checkpoint kinase; CNS, central nervous system; DHFR, dihydrofolate reductase; dTMP, deoxythymidine monophosphate; F-MTX, fluorescein methotrexate; FPGS, folylpolyglutamate synthase; GARFT, glycinamide ribonucleotide formyltransferase; MEM, minimum essential medium; MTX, methotrexate; PARP, poly(ADP-ribose) polymerase; PDX, patient-derived xenograft; PTX, pemetrexed; RFC, reduced folate carrier; RPA, replication protein A; RTX, raltitrexed; TMPK, dTMP kinase; TS, thymidylate synthase.

1 | INTRODUCTION

Neuroblastoma is a neuroendocrine tumor originating from the neural crest cells and is the most common extracranial solid tumor of childhood.[1,2] It is a rare disease with approximately 200 cases per year reported in Japan.[3] To date, several clinical staging systems have been proposed for this disease. Among them, the International Neuroblastoma Staging System is widely used as a postsurgical staging system.[2,4] Recently, the International Neuroblastoma Risk Group Staging System was proposed as a new staging system for pretreatment risk classification.[5] By combining these staging systems with other prognostic factors (eg age at diagnosis, tumor histology, and genetic aberrations), neuroblastoma patients can be classified into 4 groups: very-low-risk, low-risk, intermediate-risk, and high-risk. Although driver gene mutations are rare in neuroblastoma at diagnosis, gene amplification of *MYCN*, a member of the *MYC* gene family, is consistently associated with poor prognosis.[6] N-Myc, the gene product of *MYCN*, forms a transcriptional complex with MAX and regulates the expression of multiple target genes.[7,8] It has been reported that *MYCN* amplification is a characteristic feature of the high-risk group and that the 5-year event-free survival rate in a large patient cohort was 29%.[5]

For the treatment for high-risk neuroblastoma patients, combination chemotherapies are used as induction therapy.[2,3] The treatment regimens include alkylating agents (cyclophosphamide and ifosfamide), platinum compounds (cisplatin and carboplatin), the topoisomerase-II inhibitor etoposide, and the anthracycline THP-adriamycin. However, in addition to the low cure rates, the incidence of nephrotoxicity and bone marrow suppression associated with high-dose chemotherapy have raised serious concerns. Therefore, new therapeutic approaches for high-risk neuroblastoma patients are the need of the hour.

Although anticancer drugs targeting thymidylate (dTMP) biosynthesis pathways are widely used for cancer therapy over the past 60 years,[9] their clinical usefulness for neuroblastoma patients have not been well examined. Thymidylate synthase, a central enzyme in the "de novo" dTMP synthesis pathway, catalyzes the conversion of dUMP to dTMP, which is further phosphorylated to a triphosphate form (dTTP) by dTMP kinase (TMPK) and nucleotide diphosphate kinase (Figure S1).[10] Therefore, the inhibition of the enzymatic activity of TS by a small chemical compound leads to a dTTP deficiency, which in turn inhibits DNA synthesis in the cancer cells. At present, 5-fluorouracil, a fluorinated pyrimidine, and its prodrugs are most widely used as TS inhibitors for the treatment of colorectal and gastric cancers.[9] The second class of TS inhibitors is antifolates that are structurally similar to folates. To date, 4 antifolate drugs, MTX, PTX, RTX, and pralatrexate are approved as anticancer drugs.[9] Antifolates are incorporated into cancer cells primarily through a membrane transporter named RFC encoded by the *SLC19A1* gene (Figure S1). After entering the cell, they are polyglutamated by the FPGS and are retained within the cell. The polyglutamated forms of antifolates can inhibit the enzymatic activities of TS, DHFR, and GARFT, resulting in dTMP deficiency and subsequent imbalance in the nucleotide pool.[9] Interestingly, a recent study reported that the *MYCN*-amplified neuroblastoma cells show an enhanced folate dependence and high MTX sensitivity.[11] Because the *SLC19A1* gene is a direct transcriptional target of N-Myc, the levels of RFC protein are high in the *MYCN*-amplified cells, and therefore, the incorporation of MTX is thought to be enhanced. However, there was no direct experimental evidence that shows higher MTX uptake in the *MYCN*-amplified cell lines than in *MYCN* nonamplified cell lines. Moreover, *SLC19A1* knockdown experiments to account for the importance of RFC in their observation were not carried out. Thus, the molecular mechanisms underlying high MTX sensitivity observed in *MYCN*-amplified neuroblastoma cell lines are still unclear.

In this study, we examined the efficacies of the antifolate drugs MTX, PTX, and RTX, in *MYCN*-amplified and nonamplified neuroblastoma cell lines. We found that RTX was the most potent antifolate against the *MYCN*-amplified neuroblastoma cells. The molecular mechanisms underlying the *MYCN*-amplified cell-specific growth suppression and its clinical potential as a new treatment for high-risk neuroblastoma were discussed.

2 | MATERIALS AND METHODS

2.1 | Cell culture and reagents

SK-N-BE(2), SK-N-AS, and SH-SY5Y cells were obtained from the ATCC (USA). LAN-5 and SK-N-FI cells were obtained from the Childhood Cancer Repository (USA). NB-39, LAN-1, and SK-N-SH cells were obtained from the RIKEN BRC Cell Bank (Japan). IMR-32 cells were obtained from the JCRB Cell Bank (Japan). KELLY cells were kindly provided by Dr N. Hattori (National Cancer Center Research Institute, Tokyo, Japan). The neuroblastoma cells were cultured in a standard medium with 10% heat-inactivated FBS in a humidified atmosphere containing 5% CO_2 at 37°C. The following culture medium were used: MEM (M4655; Sigma-Aldrich) for IMR-32, SK-N-BE(2), SK-N-SH, and SH-SY5Y; RPMI-1640 (R8758, Sigma-Aldrich) for KELLY, LAN-1, LAN-5, NB-39, and SK-N-FI; and DMEM (D5796; Sigma-Aldrich) for SK-N-AS. Carboplatin (C2043) and cisplatin (D3371) were purchased from Tokyo Chemical Industry. Etoposide (E1383), RTX (R9156), methotrexate (M6770), PTX (SML1490), and thymidine (T1895) were purchased from Sigma-Aldrich.

2.2 | Cell viability assay and IC_{50} calculation

The cell growth-inhibitory activities of antifolate drugs on *MYCN*-amplified neuroblastoma cell lines (IMR-32, SK-N-BE(2), KELLY, LAN-1, LAN-5, and NB-39) and nonamplified cell lines (SK-N-AS, SK-N-FI, SK-N-SH, and SH-SY5Y) were compared. Cells were cultured in a 96-well microplate (3860-096; IWAKI) for 24 hours to permit adherence, and then treated with 0.01 nmol/L-100 μmol/L MTX, PTX, and RTX for 72 hours. At the end of the incubation time, 200 μmol/L alamarBlue solution (resazurin sodium salt, R7017; Sigma-Aldrich)

was added to each well and the plates were incubated again for 2 hours. The fluorescence was measured with excitation wavelength at 560 nm and emission wavelength at 590 nm using PoweScan4 plate reader (BioTek). The absolute IC_{50} values were calculated using GraphPad Prism 8.3.0 (GraphPad Software). The absolute IC_{50} values of etoposide, cisplatin, and carboplatin were also determined based on their growth inhibitory activity against IMR-32 and SH-SY5Y cells. These 2 well-studied cell lines were used owing to their doubling times being reportedly almost the same.[11]

2.3 | Western blot analysis and Abs

The cells were lysed with NET-N buffer[12] (20 mmol/L Tris-HCl [pH 8.0], 150 mmol/L NaCl, 1 mmol/L EDTA, and 0.5% NP-40) containing protease and phosphatase inhibitor cocktail (25955-24 and 07574-61; Nacalai Tesque). Protein concentrations were measured by using the BCA protein assay reagent (23225; Thermo Fisher Scientific). For western blotting, 5 or 10 μg total protein was subjected to SDS-PAGE and separated proteins were then transferred to the PVDF membrane (IPVH00010; Merck). The following Abs were used: N-Myc (D4B2Y) rabbit mAb (#51705; Cell Signaling Technology), reduced folate carrier/SLC19A1 Ab (NBP1-59904; Novus Biologicals), thymidylate synthase (D5B3) XP rabbit mAb (#9045; Cell Signaling Technology), DHFR rabbit polyclonal Ab (15194-1-AP; Proteintech), monoclonal anti-β-actin clone AC-15 (A5441; Sigma-Aldrich), cleaved PARP (Asp214) (D64E10) XP rabbit mAb (#5625; Cell Signaling Technology), cleaved caspase-3 (Asp175) (5A1E) rabbit mAb (#9664; Cell Signaling Technology), anti-phospho-histone H2A.X (Ser139) clone JBW301 (#05-636; Merck), phospho-Chk1/2 Ab sampler kit (#9931; Cell Signaling Technology), RPA32/RPA2 (4E4) rat mAb (#2208; Cell Signaling Technology), monoclonal mouse anti-Human p53 protein clone DO-7 (M7001; Agilent), p21 Waf1/Cip1 (12D1) rabbit mAb (#2947; Cell Signaling Technology), anti-rabbit IgG, HRP-linked antibody (#7074; Cell Signaling Technology), anti-mouse IgG, HRP-linked antibody (#7076; Cell Signaling Technology), and anti-rat IgG, HRP-linked antibody (#7077; Cell Signaling Technology). Chemiluminescent signals were detected on the Amersham Imager 680 (GE Healthcare Life Sciences). Signal intensities were quantified using the Amersham Imager 680 analysis software version 2.0.0.

2.4 | Fluorescein methotrexate assay

The fluorescein methotrexate assay was undertaken as described previously.[13,14] Briefly, *MYCN*-amplified cells (IMR-32 and KELLY) and nonamplified cells (SH-SY5Y and SK-N-FI) were seeded in a 60-mm dish (1.0×10^5 cells per dish) and cultured for 24 hours at 37°C. The culture medium was then replaced with fresh MEM containing 1-10 μmol/L F-MTX (M1198MP; Thermo Fisher Scientific), and the cells were cultured again for 2 hours. The medium was then replaced with fresh culture medium without F-MTX and incubated for 30 min at 37°C. The cells were collected, and 20 000 cells were analyzed by the Gallios flow cytometer (Beckman Coulter) with excitation at 488 nm and emission at 525 nm.

2.5 | Statistical analysis

Two-tailed Student's *t* test was used for statistical analysis. $P < .05$ was considered significant.

3 | RESULTS

To investigate drug efficacies, we determined IC_{50} values of antifolate drugs MTX, PTX, and RTX, against a series of *MYCN*-amplified and nonamplified neuroblastoma cell lines. Absolute IC_{50} values are presented in Table 1. The viabilities of the most *MYCN* nonamplified cell lines were above 50% at maximum concentration (Figure 1A). The determined IC_{50} values of MTX against neuroblastoma cell lines were comparable with those reported in a previous study.[11] Interestingly, the potencies of RTX were the highest among the antifolate drugs we tested. Furthermore, the high-level RTX resistance was observed in the *MYCN* nonamplified cell lines. This prompted us to compare the efficacy of RTX with those of anticancer drugs

TABLE 1 Status of *MYCN* and absolute IC_{50} values for methotrexate (MTX), pemetrexed (PTX), and raltitrexed (RTX) in 10 neuroblastoma cell lines

Cell line	*MYCN* status	MTX IC_{50} (nmol/L)	PTX IC_{50} (nmol/L)	RTX IC_{50} (nmol/L)
IMR-32	Amplified	34 ± 2.6	88 ± 1.8	5.7 ± 1.8
SK-N-BE(2)	Amplified	100 ± 6.7	120 ± 21	6.1 ± 2.1
KELLY	Amplified	53 ± 17	99 ± 6.4	8.9 ± 0.64
NB-39	Amplified	72 ± 6.7	130 ± 40	16 ± 3.2
LAN-5	Amplified	100 ± 4.0	290 ± 95	25 ± 7.8
LAN-1	Amplified	97 ± 1.8	> 100 000	54 ± 11
SK-N-AS	Nonamplified	210 ± 48	>100 000	>100 000
SK-N-FI	Nonamplified	>100 000	>100 000	>100 000
SK-N-SH	Nonamplified	>100 000	>100 000	>100 000
SH-SY5Y	Nonamplified	>100 000	>100 000	>100 000

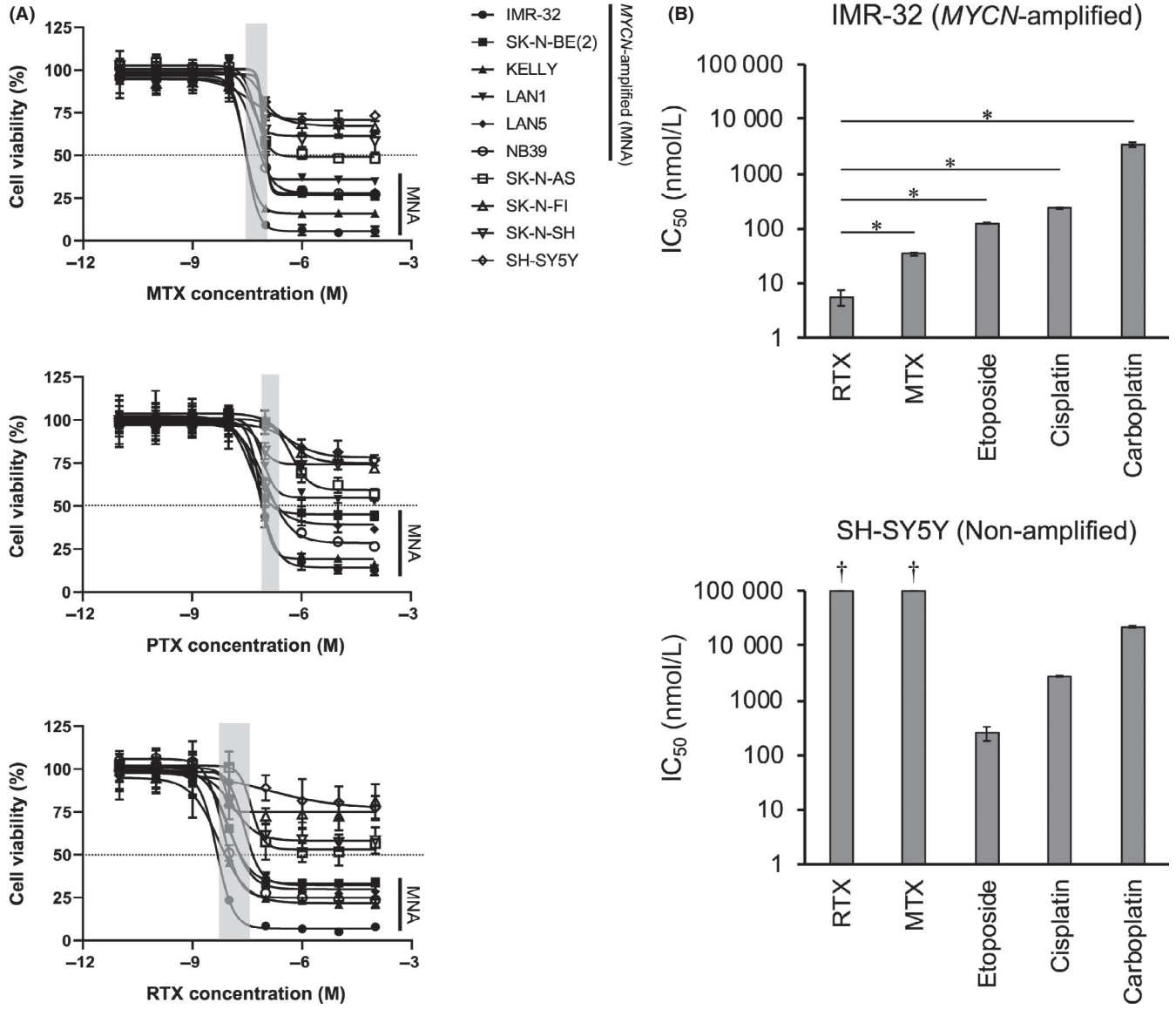

FIGURE 1 High sensitivity of *MYCN*-amplified neuroblastoma cell lines to raltitrexed (RTX). A, Dose-response curves to methotrexate (MTX), pemetrexed (PTX), and RTX at 72 hours of incubation for a panel of 6 *MYCN*-amplified (MNA) and 4 *MYCN* nonamplified neuroblastoma cell lines (mean ± SE, n = 3). The regions corresponding to IC_{50} values against MNA cell lines are marked by a light gray shading. B, IC_{50} values of RTX, MTX, etoposide, cisplatin, and carboplatin against IMR-32 (*MYCN*-amplified) and SH-SY5Y (nonamplified) cell lines (mean ± SE, n = 3). † IC_{50} > 100 μmol/L. *P<.01

used in induction therapy for high-risk neuroblastoma. As shown in Figure 1B, the efficacy of etoposide was comparable between the 2 cell lines and the calculated IC_{50} values of the 2 platinum compounds were approximately 10 times lower in the IMR-32 cells. Compared with these conventional drugs, RTX showed the highest cell growth-inhibitory activity and selectivity against the IMR-32 cells, a *MYCN*-amplified cell line. These results suggested that RTX would be one of the most beneficial compounds for the treatment of *MYCN*-amplified neuroblastoma from the viewpoints of efficacy and selectivity to *MYCN*-amplified cells.

Consistent with a previous report, our study identified that MTX was effective against a wide variety of *MYCN*-amplified neuroblastoma cell lines; however, the molecular mechanisms that enhance the efficacies of antifolates are still unclear. One possible explanation for this observation was that the N-Myc directly upregulates the expression of the RFC, the gene product of *SLC19A1*, and therefore, antifolates can be incorporated into the *MYCN*-amplified cells effectively.[11] Although the authors examined the relationship between *MYCN* and *SLC19A1* gene expression by quantitative PCR assay, the *SLC19A1* gene expression levels were almost similar among most of the cell lines tested. Moreover, the expression levels of RFC protein were not determined by western blotting. We, therefore, examined the correlation between N-Myc and RFC protein expression. The protein levels were found to be varied in different cell lines and there was no significant difference between the 2 groups (Figure 2A,B). It has been reported that the low expression of TS or DHFR is a predictive factor for a good response to antifolates.[15] As a result, in our study, high TS protein expression was observed in LAN-1 cells,

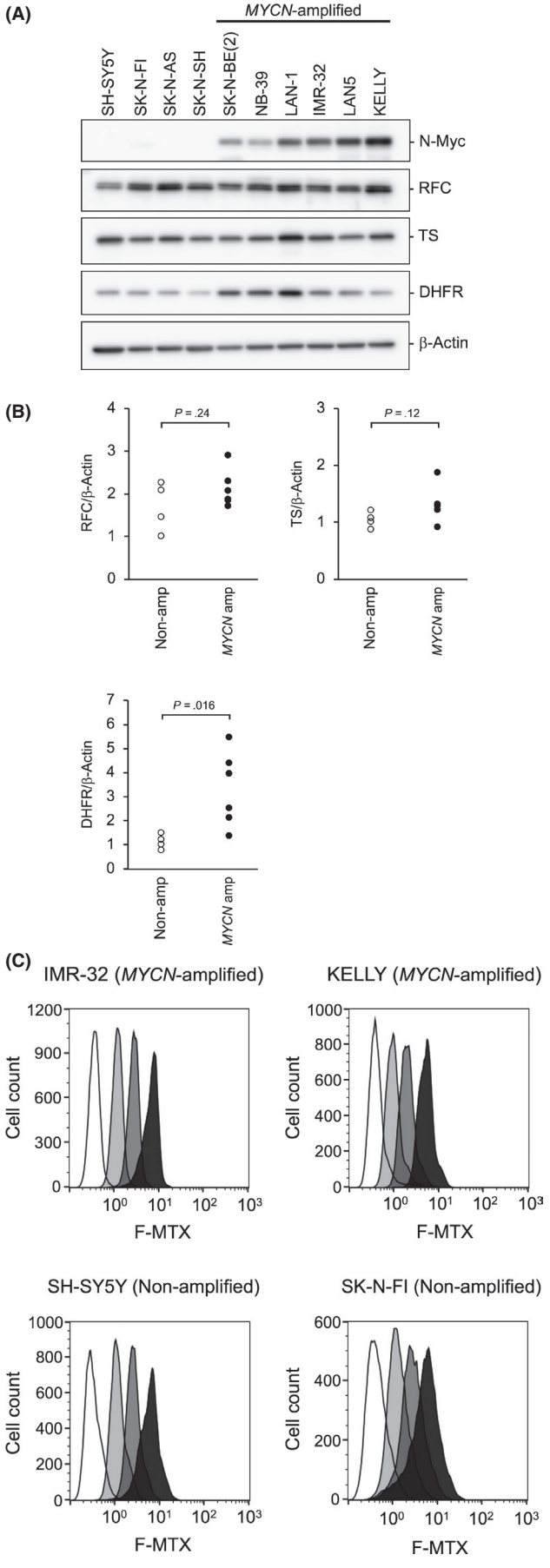

FIGURE 2 Protein expression levels of reduced folate carrier (RFC), thymidylate synthase (TS), and dihydrofolate reductase (DHFR) and their correlation with N-Myc expression. A, Cell lysates were subjected to western blot analysis with anti-N-Myc, anti-RFC, anti-TS, anti-DHFR, and anti-β-actin Abs. B, Protein expression levels of RFC, TS, and DHFR (normalized against β-actin) in 6 *MYCN*-amplified and 4 *MYCN* nonamplified (Nonamp) neuroblastoma cell lines. C, Flow cytometric analysis of fluorescein methotrexate (F-MTX) incorporation in 2 *MYCN*-amplified (IMR-32 and KELLY) and 2 *MYCN* nonamplified (SH-SY5Y and SK-N-FI) cells. Cells were incubated with 0, 1, 3, and 10 μmol/L F-MTX for 2 h and washed with fresh culture medium without F-MTX for 30 min. A total of 20 000 cells were analyzed by flow cytometer

a *MYCN*-amplified cell line; however, the protein levels of TS were almost similar among the other neuroblastoma cell lines (Figure 2B). These analyses showed that the protein levels of two key molecules, RFC and TS, were not the cause of the high selective inhibitory activity of RTX against *MYCN*-amplified cell lines. Interestingly, significantly high DHFR protein expression was observed in *MYCN*-amplified cell lines (Figure 2B).

As a next step, we sought to directly examine whether the efficiency of RTX incorporation can be affected by the *MYCN* status. Unfortunately, isotope-labeled RTX or fluorescein-labeled RTX is not commercially available; thus, we utilized F-MTX.[13,14] Because both MTX and RTX are incorporated by RFC on the cell membrane (Figure S1), it is possible to evaluate the efficiency of RTX incorporation by using F-MTX. As a result, all the cells were effectively labeled by F-MTX in a dose-dependent manner (Figure 2C). In general, the efficient excretion of MTX from the cell can be a molecular mechanism for drug resistance. We confirmed that longer washout time up to 2 hours did not affect the fluorescence intensity of SH-SY5Y cells (data not shown). As described above, MTX is polyglutamated by FPGS in the cytosol, and thus, the incorporated MTX will be retained for long periods of time. In summary, our analyses showed that MTX can be incorporated into both *MYCN*-amplified and nonamplified neuroblastoma cells to similar extent, suggesting that drug incorporation is not critical for differences in sensitivity to the antifolates.

It has been postulated that lowered cellular dTTP level arising from TS inhibition is the molecular mechanism underlying RTX activity.[9] To exclude the possibility that RTX or its metabolite can interfere with other biological pathways, particularly in *MYCN*-amplified cells, we tested whether the growth arrest was canceled by dTMP supplementation. In addition to the "de novo" synthesis of dTMP, the cells are capable of producing dTMP by the salvage pathway that is mediated by thymidine kinase (Figure 3A).[10] Because most cell culture media (exceptions include Ham's F12 and Alpha-MEM) do not contain thymidine, the salvage pathway cannot be used in cultured cells. IMR-32 cells were treated with MEM containing various concentrations of RTX in the presence of 1-10 μmol/L thymidine. As shown in Figure 3B, the growth inhibition of IMR-32 cells was rescued by thymidine supplementation (more than 3 μmol/L). This indicated that the thymidine salvage pathway was active in IMR-32

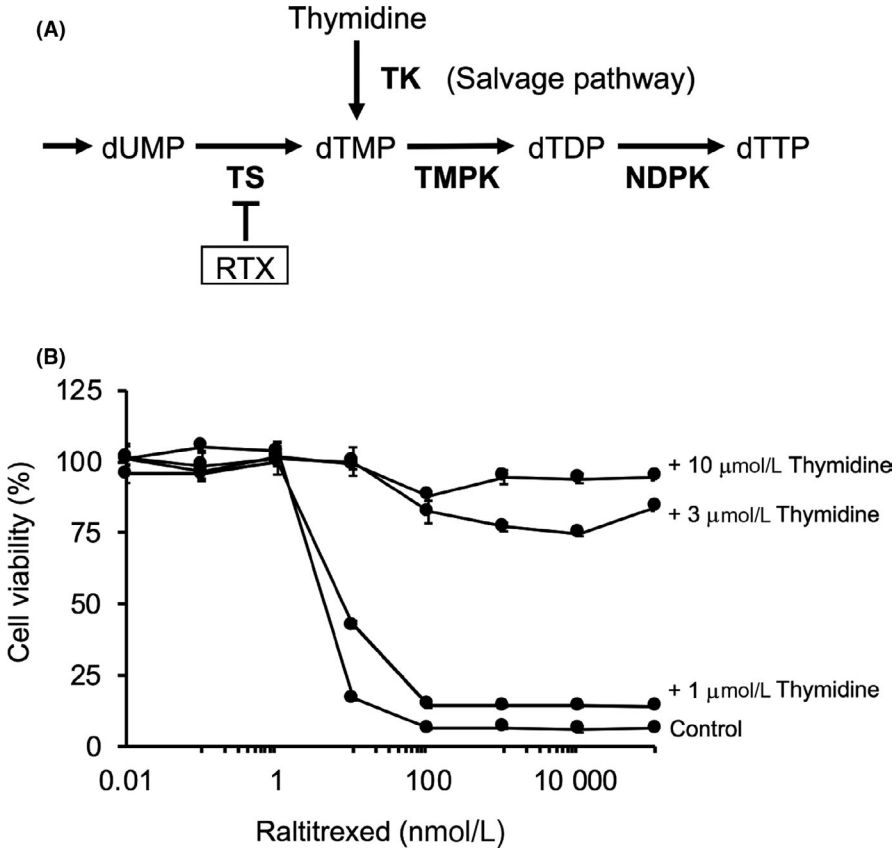

FIGURE 3 Rescue of raltitrexed (RTX)-induced cell growth suppression by thymidine supplementation. A, Salvage pathway to produce dTMP. Exogenous thymidine is phosphorylated by thymidine kinase (TK). dTMP is then phosphorylated to triphosphate form (dTTP) by dTMP kinase (TMPK) and nucleotide diphosphate kinase (NDPK). B, IMR-32 cells were treated with minimum essential medium containing various concentrations of RTX (in the presence of 0, 1, 3, and 10 μmol/L thymidine)

cells and that dTMP shortage after TS inhibition by RTX was the sole cause of the cell growth arrest.

As the next step toward understanding the mechanism of RTX-induced cell growth inhibition, we compared 2 neuroblastoma cell lines, IMR-32 and SH-SY5Y, for their cell growth rate and DNA damage response during RTX treatment. IMR-32 cells were treated with near-IC_{50} of RTX (10 nmol/L) for 72 hours. Because of their extraordinary resistance to RTX, SH-SY5Y cells were treated with an additional concentration of 10 μmol/L RTX. As shown in Figure 4A, RTX treatment affected the cell growth rate of IMR-32 cells but had a modest effect on SH-SY5Y cells. A clear suppression effect on the IMR-32 cells was observed after 48 hours of treatment, which was consistent with the increased levels of apoptotic cell death determined by western blotting for cleaved PARP and cleaved caspase-3 (Figure 4B). In addition, the accumulation of γ-H2AX, a DNA damage marker, was observed in IMR-32 cells after 48 hours of RTX treatment. A relatively low amount of γ-H2AX was detected in the SH-SY5Y cells at 72 hours. To gain further insight into the different DNA damage response to RTX, we examined the phosphorylation status of DNA damage checkpoint kinases, Chk1 and Chk2, by western blotting. As shown in Figure 4C, the peak phosphorylation of Chk1 at Ser345, which was phosphorylated by ATR kinase after the formation of single-stranded DNA,[16] was observed at 48 hours. It is widely known that RPA, a single-stranded DNA binding protein, is hyperphosphorylated by PI3K-related protein kinases (ATR, ATM, and DNA-dependent protein kinase) in response to DNA damage.[17] Consistent with this, phosphorylation of RPA2 at Ser4 and Ser8 was clearly detected after 48 hours of treatment. This was also confirmed by the high-molecular-mass smear bands of total RPA2 (Figure 4C, arrowhead). The phosphorylation of Chk2 at Thr68, which was phosphorylated by ATM kinase after DNA double-strand break,[16] was detected at 48 hours, and the phosphorylation peaked at 72 hours. Although a similar DNA damage response was observed in the SH-SY5Y cells after 72 hours of RTX treatment even at 10 nmol/L, the phosphorylation levels of Chk1 and RPA2 were relatively low. Stabilization of p53 and subsequent accumulation of p21, a potent cyclin-dependent kinase inhibitor, were observed in both cell lines at similar levels. However, the induction of apoptosis in IMR-32 cells was preceded by the p21 accumulation. These results suggest that exposure of single-stranded DNA after dTTP depletion and subsequent DNA double-strand break formation were the main causes of IMR-32 cell growth suppression by RTX.

4 | DISCUSSION

Although antifolates are widely used as anticancer drugs, their usefulness in the treatment of neuroblastoma patients has not been fully investigated. We found, for the first time, that RTX is the most potent antifolate drug to treat *MYCN*-amplified neuroblastoma cells. In contrast to the molecular mechanism proposed in a previous study,[11] MTX can be incorporated into both *MYCN*-amplified and nonamplified neuroblastoma cells with similar efficiencies, and therefore, we focused on the DNA damage response

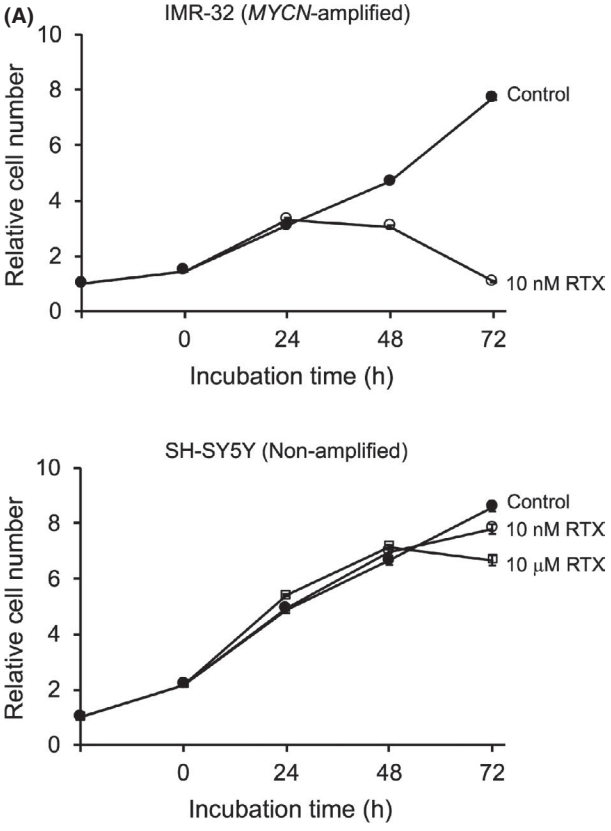

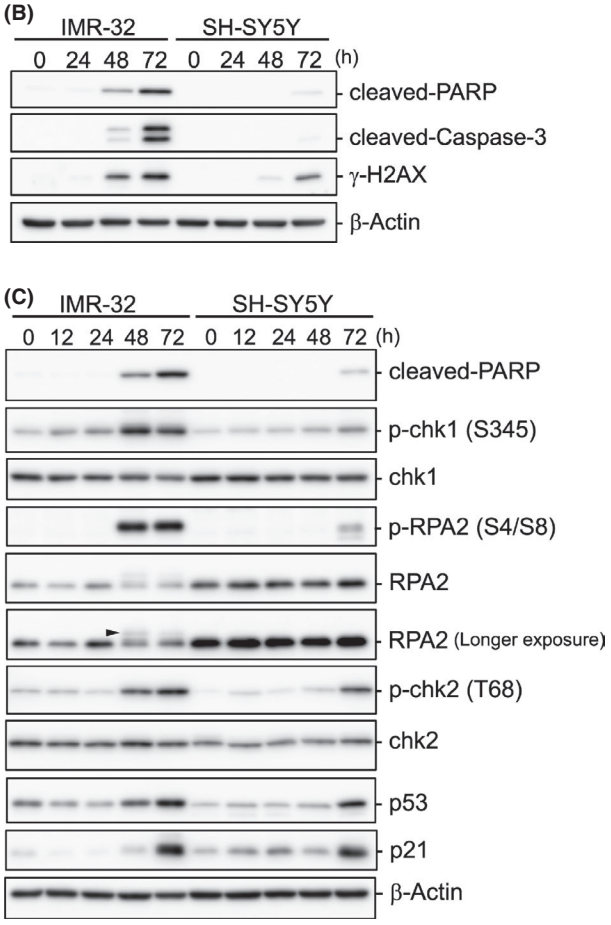

FIGURE 4 Differences in cellular response to raltitrexed (RTX) treatment. A, IMR-32 (*MYCN*-amplified) and SH-SY5Y (nonamplified) cells were treated with 10 nmol/L or 10 μmol/L RTX for 72 h. Cell numbers were determined by alamarBlue assay every 24 h. Data represent the mean of triplicate and bars show SEs. B, Detection of apoptotic cell death markers (cleaved poly(ADP-ribose) polymerase [PARP] and cleaved caspase-3) and DNA damage marker (γ-H2AX). Cells were collected every 24 h after 10 nmol/L of RTX treatment and subjected to western blotting. C, Detection of DNA damage response makers. Cells were collected every 24 h after 10 nmol/L of RTX treatment and subjected to western blotting. Arrowhead shows high-molecular-mass smear bands of total replication protein A2 (RPA2). Chk, checkpoint kinase

induced by RTX treatment. We observed apoptotic cell death in IMR-32 cells 48 hours after RTX treatment, which was coupled with γ-H2AX formation. A detailed time-course analysis revealed that single-stranded DNA formation, which was determined by Chk1 and RPA2 phosphorylation, was higher in IMR-32 cells than in SH-SY5Y cells. Subsequent dsDNA damage formation was confirmed by phosphorylated Chk2. These differences in the DNA damage response might explain the molecular mechanisms underlying RTX sensitivity observed in our experiments. It is widely known that the high levels of DNA replication stress are induced by aberrant *MYC* or *MYCN* expression.[18] Therefore, basal DNA damage levels are thought to be high in *MYCN*-amplified neuroblastoma cells. To cope with this, several DNA repair genes (eg *APEX1*, *MRE11*, and *PARP1*)

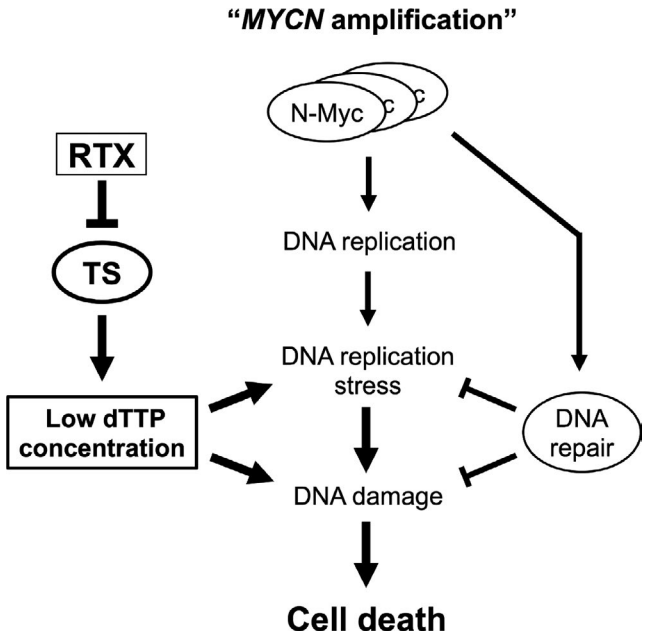

FIGURE 5 Schematic representation of the molecular mechanism of raltitrexed (RTX)-induced DNA damage and cell death. Overexpression of N-Myc promotes DNA replication, which in turn causes high levels of DNA replication stress and DNA damage. DNA replication stress is further enhanced by reduced dTTP concentration after RTX treatment, which leads to apoptotic cell death in the *MYCN*-amplified neuroblastoma cells. TS, thymidylate synthase

are upregulated by N-Myc.[8,19,20] It has generally been thought that *MYCN*-amplified neuroblastoma cells can survive by balancing accelerated DNA replication stress and enhanced DNA repair.[19] In such a condition, the cellular dTTP deficiency because of TS inhibition can induce high levels of DNA replication stress and DNA damage in *MYCN*-amplified cells. In addition, reduced levels of dTTP would inhibit the DNA repair process. For example, an adequate amount of dNTP will be required for gap-filling DNA synthesis during the DNA repair process. Accordingly, we suggest that TS inhibition induces apoptotic cell death specifically in *MYCN*-amplified neuroblastoma cells by increasing DNA damage (Figure 5).

New therapeutic approaches for high-risk neuroblastoma patients have been developed. For example, immunotherapies using anti-GD2 chimeric mAb or CAR-T are currently being evaluated.[3] To identify new therapeutic target molecules for treating *MYCN*-amplified neuroblastoma, we have undertaken a genome-wide shRNA library screening by using a commercial library comprising over 80 000 shRNA constructs targeting approximately 16 000 human genes (S. Kiyonari, unpublished data). Briefly, IMR-32 (*MYCN*-amplified) and SH-SY5Y (*MYCN* nonamplified) cells were transduced with lentiviruses carrying the shRNA sequences. The relative abundance of shRNA constructs in each cell line were then quantified by next-generation sequencing. Interestingly, the dUTPase and TMPK were identified as important molecules, especially for the IMR-32 cells. As shown in Figure S1, they play important roles in de novo dTMP biosynthesis. This finding also indicates the importance of the pathway for *MYCN*-amplified neuroblastoma cells. Thus, the development of new small molecule inhibitors against these enzymes is desirable. In fact, inhibitors against dUTPase[21] and DTYMK[22,23] are under investigation as therapeutic agents for certain types of cancer.

Our experiments cannot explain why RTX shows superior growth inhibition in *MYCN*-amplified cells. The most plausible explanation for this is that the intrinsic TS inhibitory activity of RTX is the highest among the approved antifolates. In general, the inhibition constants differ among previously reported studies because of differences in factors such as enzyme activities of purified protein, reaction conditions, and calculation methods. Therefore, we summarized inhibition constant values of the antifolates toward the recombinant TS, DHFR, and GARFT, based on the reports from the same group (Table S1).[24,25] Both MTX and RTX have weak inhibitory activity against GARFT, and their primary target is DHFR and TS, respectively. Considering that RTX showed the strongest cell growth-inhibitory activity, specific inhibition of TS would be more effective in the *MYCN*-amplified cells. In contrast, PTX has broad inhibitory activities, and therefore, it is called a "multitargeted drug".[26] In addition to these 3 enzymes, aminoimidazole-carboxamide ribonucleotide formyltransferase is also known as a molecular target of PTX. Although the inhibitory activity of RTX on the recombinant TS protein is similar to that of PTX, the cell growth-inhibitory activity of RTX is more potent than PTX. We consider that the broad spectrum of the target enzymes lowers the effective concentration of PTX against TS.

As discussed above, antifolates could have the potential to be used as an anticancer drug in *MYCN*-amplified neuroblastoma. As an important clinical application, infusion of high-dose MTX is used for treating pediatric patients with acute lymphoblastic leukemia or CNS tumors.[27,28] Basically, MTX cannot cross the BBB at low concentrations, similar to other anticancer drugs; however, the rapid i.v. infusion of high-dose MTX enables the molecule to penetrate the BBB. Because of the structural similarity of RTX to MTX,[29] it can be postulated that RTX has the potential to cross the BBB. In relation to this notion, MTX and RTX are delivered successfully to the brain by intranasal delivery.[30] Although the rate of CNS metastasis in neuroblastoma is relatively low, recent studies have suggested that the incidence of CNS recurrence is increasing.[31] Thus, elucidating the RTX treatment protocol that is well tolerated and effective for the treatment of metastatic *MYCN*-amplified neuroblastoma will be valuable to improve prognosis.

The efficacies of antifolates in human neuroblastoma xenograft models have not been reported, including the previous study that reported the usefulness of MTX.[11] As the antifolates used in this study are clinically approved drugs for the treatment of various types of cancer, they have favorable pharmacokinetic properties in nude mice. For example, the efficacies of RTX against colorectal cancer xenograft models have been reported.[32-34] The reported IC_{50} values of RTX against colorectal cancer cell lines (ranging from 5.3 to 59 nmol/L)[35] were comparable with those of *MYCN*-amplified neuroblastoma cell lines (Table 1); therefore, RTX might be effective in neuroblastoma xenograft models. Recent studies have shown that PDX models are more reliable and valuable for predicting response to cancer therapy.[36,37] Therefore, we are currently trying to establish neuroblastoma PDX models. Future research should validate the efficacy of antifolates on the PDX models and the feasibility of developing antifolate-based therapies for high-risk neuroblastoma.

ACKNOWLEDGMENTS

This work was supported by JSPS KAKENHI Grant Numbers JP15K18442 and JP19K07711.

DISCLOSURE

The authors have no conflict of interest.

ORCID

Shinichi Kiyonari https://orcid.org/0000-0002-4456-7186

REFERENCES

1. Maris JM, Hogarty MD, Bagatell R, Cohn SL. *Neuroblastoma. Lancet*. 2007;369:2106-2120.
2. Matthay KK, Maris JM, Schleiermacher G, et al. Neuroblastoma. *Nat Rev Dis Primers*. 2016;2:16078.
3. Nakagawara A, Li Y, Izumi H, Muramori K, Inada H, Nishi M. Neuroblastoma. *Jpn J Clin Oncol*. 2018;48:214-241.
4. Brodeur GM, Pritchard J, Berthold F, et al. Revisions of the international criteria for neuroblastoma diagnosis, staging, and response to treatment. *J Clin Oncol*. 1993;11:1466-1477.
5. Cohn SL, Pearson ADJ, London WB, et al. The International Neuroblastoma Risk Group (INRG) classification system: an INRG Task Force report. *J Clin Oncol*. 2009;27:289-297.

6. Brodeur GM. Neuroblastoma: biological insights into a clinical enigma. *Nat Rev Cancer*. 2003;3:203-216.
7. Boon K, Caron HN, van Asperen R, et al. N-myc enhances the expression of a large set of genes functioning in ribosome biogenesis and protein synthesis. *EMBO J*. 2001;20:1383-1393.
8. Valentijn LJ, Koster J, Haneveld F, et al. Functional MYCN signature predicts outcome of neuroblastoma irrespective of MYCN amplification. *Proc Natl Acad Sci USA*. 2012;109:19190-19195.
9. Wilson PM, Danenberg PV, Johnston PG, Lenz H-J, Ladner RD. Standing the test of time: targeting thymidylate biosynthesis in cancer therapy. *Nat Rev Clin Oncol*. 2014;11:282-298.
10. Mathews CK. Deoxyribonucleotide metabolism, mutagenesis and cancer. *Nat Rev Cancer*. 2015;15:528-539.
11. Lau DT, Flemming CL, Gherardi S, et al. MYCN amplification confers enhanced folate dependence and methotrexate sensitivity in neuroblastoma. *Oncotarget*. 2015;6:15510-15523.
12. Peng M, Litman R, Xie J, Sharma S, Brosh RM, Cantor SB. The FANCJ/MutLalpha interaction is required for correction of the cross-link response in FA-J cells. *EMBO J*. 2007;26:3238-3249.
13. Santiago Y, Chan E, Liu P-Q, et al. Targeted gene knockout in mammalian cells by using engineered zinc-finger nucleases. *PNAS*. 2008;105:5809-5814.
14. Liu P-Q, Chan EM, Cost GJ, et al. Generation of a triple-gene knockout mammalian cell line using engineered zinc-finger nucleases. *Biotechnol Bioeng*. 2010;106:97-105.
15. Zhang Q, Shen J, Wang H, et al. TS mRNA levels can predict pemetrexed and raltitrexed sensitivity in colorectal cancer. *Cancer Chemother Pharmacol*. 2014;73:325-333.
16. Bartek J, Lukas J. Chk1 and Chk2 kinases in checkpoint control and cancer. *Cancer Cell*. 2003;3:421-429.
17. Byrne BM, Oakley GG. Replication protein A, the laxative that keeps DNA regular: the importance of RPA phosphorylation in maintaining genome stability. *Semin Cell Dev Biol*. 2019;86:112-120.
18. Dominguez-Sola D, Gautier J. MYC and the control of DNA replication. *Cold Spring Harb Perspect Med*. 2014;4:a014423.
19. Petroni M, Sardina F, Infante P, et al. MRE11 inhibition highlights a replication stress-dependent vulnerability of MYCN-driven tumors. *Cell Death Dis*. 2018;9:895-912.
20. Colicchia V, Petroni M, Guarguaglini G, et al. PARP inhibitors enhance replication stress and cause mitotic catastrophe in MYCN-dependent neuroblastoma. *Oncogene*. 2017;36:4682-4691.
21. Saito K, Nagashima H, Noguchi K, et al. First-in-human, phase I dose-escalation study of single and multiple doses of a first-in-class enhancer of fluoropyrimidines, a dUTPase inhibitor (TAS-114) in healthy male volunteers. *Cancer Chemother Pharmacol*. 2014;73:577-583.
22. Hu C-M, Yeh M-T, Tsao N, et al. Tumor cells require thymidylate kinase to prevent dUTP incorporation during DNA repair. *Cancer Cell*. 2012;22:36-50.
23. Liu Y, Marks K, Cowley GS, et al. Metabolic and functional genomic studies identify deoxythymidylate kinase as a target in LKB1-mutant lung cancer. *Cancer Discov*. 2013;3:870-879.
24. Shih C, Chen VJ, Gossett LS, et al. LY231514, a pyrrolo[2,3-d]pyrimidine-based antifolate that inhibits multiple folate-requiring enzymes. *Cancer Res*. 1997;57:1116-1123.
25. Shih C, Habeck LL, Mendelsohn LG, Chen VJ, Schultz RM. Multiple folate enzyme inhibition: mechanism of a novel pyrrolopyrimidine-based antifolate LY231514 (MTA). *Adv Enzyme Regul*. 1998;38:135-152.
26. Adjei AA. Pemetrexed (Alimta): a novel multitargeted antifolate agent. *Expert Rev Anticancer Ther*. 2003;3:145-156.
27. Bernstock JD, Alva E, Cohen JL, et al. Treatment of pediatric high-grade central nervous system tumors with high-dose methotrexate in combination with multiagent chemotherapy: a single-institution experience. *Pediatr Blood Cancer*. 2019;18:e28119.
28. Huang Z, Tong H-F, Li Y, et al. Effect of the polymorphism of folylpolyglutamate synthetase on treatment of high-dose methotrexate in pediatric patients with acute lymphocytic leukemia. *Med Sci Monit*. 2016;22:4967-4973.
29. Walling J. From methotrexate to pemetrexed and beyond. A review of the pharmacodynamic and clinical properties of antifolates. *Invest New Drugs*. 2006;24:37-77.
30. Triarico S, Maurizi P, Mastrangelo S, Attinà G, Capozza MA, Ruggiero A. Improving the brain delivery of chemotherapeutic drugs in childhood brain tumors. *Cancers (Basel)*. 2019;11:824.
31. Matthay KK, Brisse H, Couanet D, et al. Central nervous system metastases in neuroblastoma: radiologic, clinical, and biologic features in 23 patients. *Cancer*. 2003;98:155-165.
32. Jackman AL, Boyle FT, Harrap KR. Tomudex (ZD1694): from concept to care, a programme in rational drug discovery. *Invest New Drugs*. 1996;14:305-316.
33. Kabeshima Y, Kubota T, Watanabe M, et al. A potential important role for thymidylate synthetase inhibition on antitumor activity of fluoropyrimidine and raltitexed. *Anticancer Res*. 2002;22:3245-3252.
34. Qiu C, Li Y, Liang X, et al. A study of peritoneal metastatic xenograft model of colorectal cancer in the treatment of hyperthermic intraperitoneal chemotherapy with Raltitrexed. *Biomed Pharmacother*. 2017;92:149-156.
35. van Triest B, Pinedo HM, van Hensbergen Y, et al. Thymidylate synthase level as the main predictive parameter for sensitivity to 5-fluorouracil, but not for folate-based thymidylate synthase inhibitors, in 13 nonselected colon cancer cell lines. *Clin Cancer Res*. 1999;5:643-654.
36. Zarzosa P, Navarro N, Giralt I, et al. Patient-derived xenografts for childhood solid tumors: a valuable tool to test new drugs and personalize treatments. *Clin Transl Oncol*. 2017;19:44-50.
37. Tentler JJ, Tan AC, Weekes CD, et al. Patient-derived tumour xenografts as models for oncology drug development. *Nat Rev Clin Oncol*. 2012;9:338-350.

SUPPORTING INFORMATION

Additional supporting information may be found online in the Supporting Information section.

How to cite this article: Yamashita K, Kiyonari S, Tsubota S, Kishida S, Sakai R, Kadomatsu K. Thymidylate synthase inhibitor raltitrexed can induce high levels of DNA damage in *MYCN*-amplified neuroblastoma cells. *Cancer Sci*. 2020;111:2431–2439. https://doi.org/10.1111/cas.14485